Multi-scale assessment of a grassland productivity model

Shawn D. Taylor[1] and Dawn M. Browning[1]

[1]U.S. Department of Agriculture, Agricultural Research Service, Jornada Experimental Range, New Mexico State University, Las Cruces, New Mexico, United States

Correspondence: Shawn D. Taylor (shawn.taylor@usda.gov)

Abstract. Grasslands provide a large amount of ecosystem services globally and forecasting grassland productivity in the coming decades will provide valuable information to land managers. Productivity models can be well-calibrated at local scales, but generally have some maximum spatial extent in which they perform well. Here we evaluate a grassland productivity model to find the optimal spatial extent for parameterization, and thus for subsequently applying it in future forecasts for North America. We also evaluated the model on new vegetation types to ascertain its potential generality. We find the model most suitable when incorporating only grasslands, as opposed to also including agriculture and shrublands, and only in the Great Plains and Eastern Temperate Forest ecoregions of North America. The model was not well suited to grasslands in North American Deserts or Northwest Forest ecoregions. It also performed poorly in agriculture vegetation, likely due to management activities, and shrubland vegetation, likely because the model lacks representation of deep water pools. This work allows us to perform long-term forecasts in areas where model performance has been verified, with gaps filled in by future modelling efforts.

1 Introduction

Grassland systems span nearly 30% of the global land surface (Adams et al., 1990) and play a prominent role in terrestrial carbon cycles (Parton et al., 2012). Grasslands in North America provide a large proportion of food and fiber agricultural products for the region. Annual productivity of grasslands in central and western North America is driven in large part by precipitation (Sala et al., 2012). Future changes in the amount, intensity, and timing of precipitation will be heterogeneous across North America (Easterling et al., 2017), resulting in heterogeneous changes to grassland productivity. For example, even with consistent shifts in climate, different locations can experience different changes in productivity due to local-scale responses (Zhang et al., 2011; Sala et al., 2012; Knapp et al., 2017). This highlights the need for models which can be resolved at small spatial and temporal scales, thus making long-term grassland productivity forecasts as informative as possible.

There are several potential limitations in the underlying productivity models which can drive such a forecast. Process-based models parameterized with observed data have limited transferability beyond the spatial extent from which their training data came (Taylor et al., 2019). For any location the most accurate model will be one which was parameterized from locally col-

lected data, yet these site-specific models will not generalize to new locations (Basler, 2016). Incorporating more, and diverse, locations into the model building process will allow it to be more generalizable, yet this comes at a cost of decreased proficiency at all locations (García-Mozo et al., 2008; Basler, 2016). Thus there is an optimal extent in the building and subsequent application of productivity models, which depends on a tradeoff between proficiency at the local scale and applicability at the larger scale.

Here we evaluate a productivity model with the intention of it driving long-term forecasts. The PhenoGrass model developed by Hufkens et al. (2016) is a pulse-response productivity model with temperature and precipitation as the primary drivers. The model is parameterized using observations from the Phenocam network, which have a small resolution (footprints of < 1ha), sub-daily sampling and sites across all major biomes. These attributes make the PhenoGrass model potentially widely applicable. We expand on the evaluation of the original study by using 445 additional site-years of data from 77 new sites. We test the model's performance across varying combinations of North American ecoregions and vegetation types to find an optimal spatial extent in which to parameterize and apply the model. Finally we address where the model performs poorly and how productivity forecasts for these areas could be implemented or improved.

2 Methods

2.1 PhenoGrass Model

The PhenoGrass model is an ecohydrology model which has interacting state variables for soil water, plant available water, and plant fractional cover (Hufkens et al., 2016). Model inputs are daily precipitation, temperature, potential evapotranspiration (derived from the Hargreaves equation, Hargreaves and Samani (1985)), and solar radiation. The primary output is fractional vegetation cover. The original model form, derived in Choler et 2010 and Choler et al. 2011, used only temperature and potential evapotranspiration and was parameterized using satellite-derived NDVI data. Hufkens et al. (2016) expanded on the original Choler model by incorporating growth and senescence restraints from temperature and solar radiation, and also included a scaling factor to convert Phenocam G_{cc} data to a fractional cover estimate. Hufkens et al. (2016) evaluated the PhenoGrass model using 14 grassland Phenocam sites across Western North America with a total of 34 site years. They found the modelled fractional cover correlated well with annual productivity at both a daily and annual timescale.

2.2 Phenocam Data

The Phenocam network is a global network of fixed, near-surface cameras capturing true-color images of vegetation throughout the day (Richardson et al., 2018a). Using a ratio of the three RGB bands a greenness metric (green chromatic coordinate, G_{cc}) is calculated from each image, resulting in a daily scale time series of canopy greeness. G_{cc} is a unitless metric which is highly correlated with satellite derived NDVI (Richardson et al., 2018b) and flux tower derived primary productivity (Yan et al., 2019; Toomey et al., 2015). Each Phenocam image is subset to one to several different plant vegetation types based on the field of

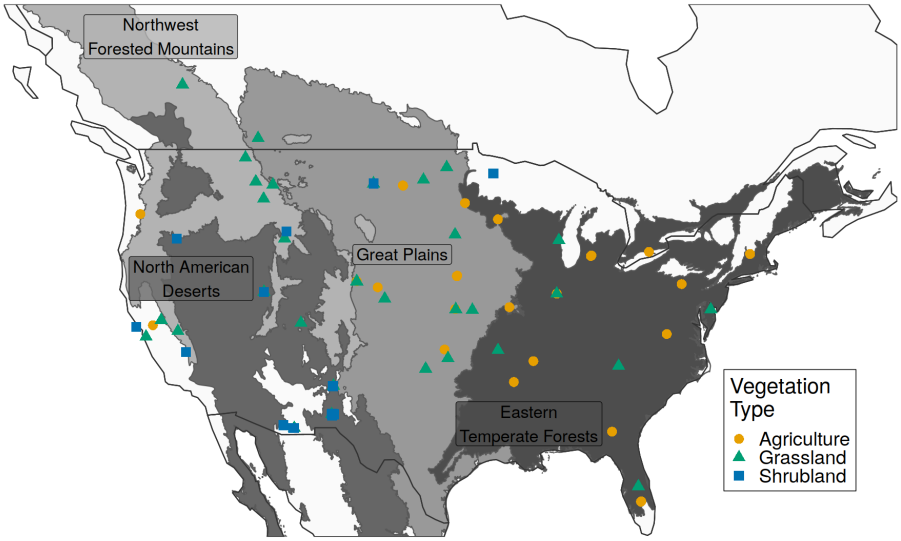

Figure 1. Locations of Phenocam sites. Color indicates the vegetation type represented at each site. Vegetation type is defined by the PhenoCam Network. Shading indicates E.P.A. North American Level 1 Ecoregions.

view. These regions of interest (ROI) serve as the basis for the G_{cc} calculation and subsequent post-processing (Seyednasrollah et al., 2019).

We downloaded all Phenocam data with ROIs of the grasslands (GR), shrublands (SH), and agricultural (AG) vegetation types for the years 2012 to 2018, totalling 91 sites and 479 site-years (Fig. 1, Table A1). As input to the PhenoGrass model we used the 3-day smoothed G_{cc} scaled, for each ROI, from 0-1. In the model parameterization each ROI time series is further transformed to a fractional cover estimate using the local mean annual precipitation (MAP) combined with a scaling factor (Hufkens et al., 2016; Donohue et al., 2013).

2.3 Environmental Data

For historic precipitation and temperature we used the daily 4-km resolution Daymet dataset (Thornton et al., 2018). Climate time series were extracted for the pixel at the location of each phenocam tower. Daily mean temperature was calculated as the average between the Daymet daily minimum and maximum temperature, and smoothed with a 15 day moving average. Potential evapotranspiration was calculated using the Hargreaves equation (Hargreaves and Samani, 1985). Soil wilting point and field capacity were extracted at each Phenocam location from a global dataset (Global Soil Data Task Group, 2000).

2.4 Model Evaluation

We used a three-step process to evaluate the PhenoGrass model at different spatial extents. First, we parameterized a suite of 15 PhenoGrass models comprising four different extents to find the most appropriate one to make forecasts (Fig. 2). The largest extent used all Phenocam locations described above (84 sites). Next were all sites, respectively, within the three vegetation types (grasslands, shrublands, and agricultural), and all sites, respectively, within each of the four ecoregions (North American Deserts, Great Plains, NW Forests, Eastern Temperate Forests) (Omernik and Griffith, 2014). Finally, we parameterized models for each vegetation type within each ecoregion (eg. All grassland locations within the Great Plains ecoregion). All sets of parameterized models were limited to have at least five sites.

Second, using the same combinations of sites described above, we applied each model parameterization to its respective extent as well as each one below it. For example, sites within the grassland vegetation type were tested using the grassland only model as well as the all site model. All sites within the Great Plains ecoregion were tested using the Great Plains ecoregion model as well as the all site model. The shrubland vegetation sites within the N.A. Deserts ecoregion were tested using its respective model, the N.A. Deserts ecoregion model, and the all site model. There was no cross-validation using out of sample data in this step as it would have been computationally expensive. Rather, error metrics from these in-sample tests were treated as a best case scenario in what each model parameterization can achieve. From these results we used a threshold to select which model to evaluate further using cross-validation at the appropriate scale. For the error metric we chose the coefficient of determination (R^2) calculated for each site, and averaged across all sites in the respective evaluation. We used a threshold of 0.65, which is viewed as "acceptable" for time-series models (Ritter and Muñoz-Carpena, 2013).

Third, models which exceed the threshold described above were subject to further evaluation. For each model we performed a leave one out cross-validation, where the model was re-fit with one Phenocam site not included in the training data, and then evaluated against the left out site. In this step a scaling coefficient to link mean annual precipitation with PhenoCam G_{cc} was held constant at the value obtained in step two. The resulting coefficient of determination is the average among all modelled sites using their respective out of sample test.

All phenocam data was downloaded using the phenocamr R package (Hufkens et al., 2018). Other packages used in the R 3.6 language were dplyr (Wickham et al., 2017), tidyr (Wickham and Henry, 2018), ggplot2 (Wickham, 2016), daymetr (Hufkens et al., 2018), rgdal (Bivand et al., 2019), and sf (Pebesma, 2018). Python 3.7 packages included scipy (Virtanen et al., 2020), numpy (van der Walt et al., 2011), pandas (McKinney, 2010), and dask (Team, 2016). All code and data used in the analysis is available in the repository at https://github.com/sdtaylor/PhenograssReplication, the PhenoGrass model is implemented in a python package https://github.com/sdtaylor/GrasslandModels. Both are archived permanently on Zenodo (https://doi.org/10.5281/zenodo.3897319).

3 Results

At the largest extent, where the phenograss model was parameterized using all 91 sites, the model performed poorly with an average R^2 value among sites of 0.33. The error of this largest extent model when applied across different subsets of sites

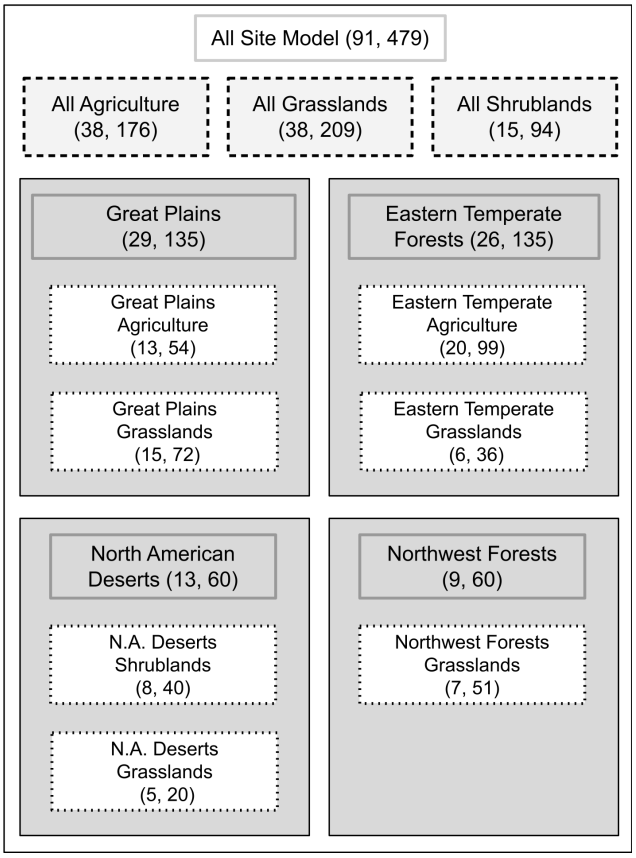

Figure 2. Scaling representation of the 15 model parameterizations. Numbers in parentheses represent the number of sites and site years, respectively. Each model uses a different subset of sites ranging from the entire dataset (All Site Model) to one vegetation type within an ecoregion (e.g., Eastern Temperate Forest Grasslands).

(Table 1, leftmost column) shows that agricultural and North American desert sites contribute most to this low R^2, while some grassland sites performed well in this regard. Models built at the ecoregion or vegetation type extent also performed poorly overall. The best model performance was achieved when models were built using a single vegetation type subset to a single ecoregion.

The grassland vegetation type, subset to specific ecoregions, predominantly outperformed other iterations of the PhenoGrass model (Table 1). Models built using grasslands within the Eastern Temperate Forest and Great Plains ecoregions had the highest average R^2 values of 0.82 and 0.70, respectively. Using leave one out cross-validation on these two grassland model iterations resulted in similar errors of 0.78 and 0.67 for the Eastern Temperate Forest and Great Plains, respectively. Grasslands in the North American deserts were not modelled well at any extent and had the lowest R^2 values in the entire analysis.

Table 1. Average site-level coefficient of determination (R^2) for each vegetation type and ecoregion group parameterized model applied to its respective extent as well as appropriate smaller extents. Bold indicates when a R^2 was greater than the "acceptable" threshold of 0.65. Values in parentheses represent the average R^2 in leave-1-out cross validation.

	All Site Model	Ecoregion Model	Vegetation Model	Ecoregion+Vegetation Model
All Sites	0.33			
E. Temperate Forests	0.43	0.48		
Agriculture	0.34	0.39	0.38	0.33
Grasslands	**0.73**	**0.79**	**0.65**	**0.82 (0.78)**
Great Plains	0.45	0.45		
Agriculture	0.22	0.15	0.17	0.18
Grasslands	0.64	**0.70**	**0.67**	**0.70 (0.67)**
N. American Deserts	-0.11	0.14		
Grasslands	-0.51	-0.22	-0.51	-0.08
Shrublands	0.15	0.37	0.40	0.51
N.W. Forests	0.25	0.58		
Grasslands	0.30	0.61	0.36	0.64
All Agriculture	0.27		0.26	
All Grasslands	0.43		0.45	
All Shrublands	0.23		0.39	

Agriculture and shrubland sites were poorly modelled at all extents. The highest average R^2 at any extent was 0.51, and 0.39 for shrubland and agriculture, respectively. Shrublands in North American Deserts improved as the model became more and more localized, but never exceeded the 0.65 threshold.

4 Discussion

We performed an extensive evaluation of the PhenoGrass model across ecoregions and vegetation types to determine the best extent at which to parameterize and apply the model. We found the model most suitable to grassland vegetation when constrained to the ecoregion level, though it did not perform well in grasslands in the North American desert ecoregion. Shrublands and agriculture were not well represented by the model regardless of the extent. Results from this study will facilitate long-term forecasts of grassland productivity constrained to an appropriate vegetation type and extent.

The PhenoGrass model performed best in grassland sites embedded within ecoregions. Studies using earlier forms of the model applied it exclusively to grasslands (Choler et al., 2010, 2011; Hufkens et al., 2016), and results here confirm that it performs well in grassland vegetation with two exceptions. The model did not work in the desert grasslands, nor did it generalize well when built using all North American grasslands simultaneously. Grasslands in the N.A. Desert biome coexist with shrubs,

resulting in complex water usage dynamics described in more detail below. The pulse-response design of PhenoGrass, which makes it well suited in areas with high cover of perennial grass, is likely not applicable when grasses are interspersed with woody plants.

Shrublands were not well modelled at any extent. Dryland shrubs, representing 8 of the 15 shrubland Phenocams analysed here, coexist with grasses by accessing different pools of soil water (Weltzin and McPherson, 2000; Muldavin et al., 2008), thus have different responses to precipitation and resulting greenness patterns (Browning et al., 2017; Yan et al., 2019). A prior form of the PhenoGrass model was designed to work with dryland shrubs (Ogle and Reynolds, 2004), yet here PhenoGrass showed little effectiveness. The current model form has only a single soil water pool with fluxes from precipitation and evapotranspiration, thus is not well-suited for representing the deeper water pools which shrubs use. Potential improvements would likely need to incorporate a deep soil water pool, in addition to the shallow, which are each utilized by the respective plant functional groups. This has already been implemented in highly parameterized ecohydrology models (Scanlon et al., 2005; Lauenroth et al., 2014) and could potentially be used here to make a more generalized PhenoShrub model to apply across large scales. This approach could also help in modelling N.A. Desert grasslands which coexist among shrubs.

Agriculture areas performed poorly with the PhenoGrass model. Management practices of crops artificially increase productivity beyond what would naturally occur, and planting and harvest result in abrupt changes in greenness metrics (Bégué et al., 2018). While the results here are unsurprising, to our knowledge this is the first attempt to use near-surface images to drive an agricultural productivity model. We have shown that the PhenoGrass model, designed for natural systems, does not generalize to managed agriculture crops. Future work in using Phenocam data to model agricultural productivity would likely need to incorporate crop specific parameters and management activity, which other cropland modelling systems use (Fritz et al., 2019). The integration of the Phenocam network within the Long-Term Agricultural Research (LTAR) will likely be beneficial for this, as the timing and intensity of management activities or experimental treatments can be incorporated into modelling efforts.

Hufkens et al. (2016) originally evaluated the Phenograss model using 14 grassland sites distributed among seven North American ecoregions. In their evaluation they had an average R^2 of 0.71, while here the model performed poorly when using more than 1 ecoregion. It's likely that the original 14 grassland sites were ideal locations for the PhenoGrass model, since on average they have a single greenup season every year in the spring or summer (Fig. 3A). The additional 24 grassland sites used in the current study have high seasonal variability and elongated growing seasons (Fig. 3B), and were thus more difficult to represent in a single continental scale grassland model.

5 Conclusions

Replication is an important step in the scientific process, especially given newly available data. Here we have validated prior modelling work and highlighted its limitations. Newer small scale vegetation models can be validated in the same framework and applied to areas where PhenoGrass performs poorly. This can result in a spatial ensemble where the output for any one location and vegetation type is represented by the most appropriate model. Our current work will allow for long-term small scale forecasts of grassland productivity for a large fraction of North America.

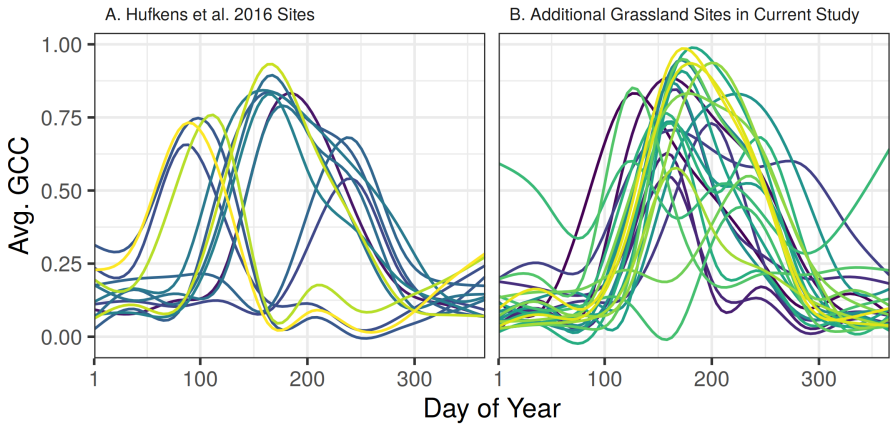

Figure 3. Smoothed time series for all 14 grassland sites used in Hufkens et al 2016 (A) and 24 additional grassland sites added in the current study (B). Each line represents the long-term average Green Chromatic Coordinate of a single site across all available years, smoothed using a GAM model.

Code and data availability. All code and data used in the analysis is available in the repository at https://github.com/sdtaylor/PhenograssReplication, the PhenoGrass model is implemented in a python package https://github.com/sdtaylor/GrasslandModels. Both are archived permanently on Zenodo (https://doi.org/10.5281/zenodo.3897319).

Appendix A: Tables in Appendix

Author contributions. Shawn concieved of the project. Shawn and Dawn wrote the paper.

Competing interests. The authors declare no competing interests.

Acknowledgements. None

Table A1. Sites used in analysis. A * indicates the site was also used in the original analysis.

name	lat	lon	vegetation	roi id	first date	last date	site years	ecoregion
ahwahnee	37.75	-119.58	GR	3000	2015-07-28	2020-03-05	4.6	NWForests
archboldavir	27.18	-81.22	AG	1000	2016-11-18	2020-03-05	3.1	ETempForests
archboldavirx	27.17	-81.22	AG	1000	2016-05-16	2020-03-05	3.6	ETempForests
archboldpnot	27.19	-81.20	AG	1000	2016-05-13	2020-03-05	3.6	ETempForests
archboldpnotx	27.18	-81.20	AG	1000	2016-05-16	2020-03-05	3.6	ETempForests
arsgacp1	31.51	-83.62	AG	1000	2016-05-10	2020-03-05	3.8	ETempForests
arsmnswanlake1	45.68	-95.80	AG	1000	2015-10-02	2020-03-05	4.4	GrPlains
bullshoals	36.56	-93.07	GR	1000	2013-11-19	2020-03-05	5.8	ETempForests
burnssagebrush	43.47	-119.69	SH	1000	2012-10-13	2020-03-05	7.3	NADeserts
butte*	45.95	-112.48	GR	1000	2009-01-11	2020-03-05	10.7	NWForests
cperagm	40.84	-104.77	AG	1000	2016-05-19	2020-03-05	3.8	GrPlains
cperagm	40.84	-104.77	GR	1000	2016-05-19	2020-03-05	3.8	GrPlains
cpertgm	40.83	-104.76	GR	1000	2016-05-04	2020-03-05	3.8	GrPlains
cperuvb	40.81	-104.76	GR	1000	2015-07-16	2020-03-05	4.7	GrPlains
gatesofthemountains	46.83	-111.71	GR	2000	2011-08-12	2019-02-01	7.1	NWForests
glacier	48.50	-113.99	GR	1000	2009-02-07	2020-03-05	11.0	NWForests
goodwater	39.23	-92.12	AG	1001	2015-09-26	2020-03-05	4.5	GrPlains
grandteton	43.92	-110.58	SH	1000	2015-07-28	2020-02-04	3.5	NWForests
harvardfarmnorth	42.52	-72.18	AG	1000	2015-11-07	2020-03-05	4.3	NForest
harvardfarmsouth	42.52	-72.18	AG	1000	2015-11-07	2020-03-05	4.3	NForest
harvardgarden	42.53	-72.19	AG	1000	2016-06-12	2020-03-05	3.7	NForest
hawbeckereddy	40.66	-77.85	AG	1000	2015-09-23	2019-05-14	3.4	ETempForests
humnokericea	34.59	-91.75	AG	1000	2015-06-25	2020-03-05	4.2	ETempForests
humnokericec	34.59	-91.75	AG	1000	2015-06-25	2020-03-05	4.5	ETempForests
ibp*	32.59	-106.85	GR	1000	2014-02-16	2020-03-05	6.0	NADeserts
ibp*	32.59	-106.85	SH	1001	2014-02-16	2020-03-02	6.0	NADeserts
jasperridge*	37.40	-122.22	GR	1000	2012-03-08	2017-03-09	5.0	MWCoastForests
jasperridge*	37.40	-122.22	GR	2000	2017-03-18	2020-03-05	3.0	MWCoastForests
jerbajada	32.58	-106.63	SH	1000	2014-04-20	2020-03-05	5.9	NADeserts
jernort	32.62	-106.79	SH	2000	2016-10-28	2020-03-05	3.3	NADeserts
jersand	32.52	-106.80	SH	1000	2014-02-28	2020-03-05	6.0	NADeserts
kansas*	39.06	-95.19	GR	1000	2012-12-03	2019-12-31	6.7	GrPlains
kaweah	36.44	-118.91	SH	1000	2011-07-13	2019-09-20	8.2	MedCA
kelloggcorn	42.44	-85.32	AG	1000	2014-05-23	2019-10-05	4.9	ETempForests

Table A2. Sites used continued

name	lat	lon	vegetation	roi id	first date	last date	site years	ecoregion
kelloggcorn2	42.40	-85.38	AG	1000	2015-07-16	2019-04-11	3.2	ETempForests
kelloggcorn3	42.40	-85.37	AG	1000	2015-07-16	2020-03-05	3.7	ETempForests
kelloggcornsoy2	42.40	-85.37	AG	1000	2015-07-16	2020-03-05	3.7	ETempForests
kelloggmiscanthus	42.40	-85.38	AG	1000	2015-07-16	2020-03-05	3.7	ETempForests
kelloggoldfield	42.40	-85.37	AG	1000	2015-07-16	2020-03-05	4.2	ETempForests
kendall*	31.74	-109.94	GR	1000	2012-07-06	2020-03-05	7.6	SouthAridHighliands
kendall*	31.74	-109.94	SH	1000	2012-08-08	2019-11-07	7.2	SouthAridHighliands
konza*	39.08	-96.56	GR	1000	2012-03-17	2019-12-19	6.2	GrPlains
lethbridge*	49.71	-112.94	GR	1000	2011-12-07	2020-03-05	8.3	GrPlains
luckyhills	31.74	-110.05	SH	2000	2015-01-26	2018-06-04	3.4	SouthAridHighliands
mandanh5	46.78	-100.95	AG	1000	2015-09-17	2020-03-05	4.5	GrPlains
mandani2	46.76	-100.93	AG	1000	2016-04-22	2020-03-05	3.7	GrPlains
manilacotton	35.89	-90.14	AG	1000	2016-06-21	2020-03-05	3.6	ETempForests
marena*	36.06	-97.21	GR	1000	2012-06-12	2018-06-19	5.8	GrPlains
mead1	41.17	-96.48	AG	1000	2016-07-12	2020-03-05	3.7	GrPlains
mead2	41.16	-96.47	AG	1000	2016-07-12	2020-03-05	3.6	GrPlains
mead3	41.18	-96.44	AG	1000	2016-07-12	2020-03-05	3.7	GrPlains
meadpasture	41.14	-96.46	AG	1000	2016-07-15	2020-03-05	3.7	GrPlains
monture*	47.02	-113.13	GR	2000	2010-11-04	2019-02-01	8.0	NWForests
mtrobson	53.03	-119.20	GR	1000	2015-02-16	2020-03-05	4.8	NWForests
nationalelkrefuge	43.49	-110.74	GR	1000	2015-08-12	2020-03-05	4.5	NWForests
NEON.D03.DSNY.	28.13	-81.44	GR	1000	2016-12-15	2020-03-05	3.2	ETempForests
NEON.D06.KONA.	39.11	-96.61	AG	1000	2016-05-07	2020-03-05	3.7	GrPlains
NEON.D06.KONZ.	39.10	-96.56	GR	1000	2017-02-25	2020-03-05	3.0	GrPlains
NEON.D09.WOOD.	47.13	-99.24	GR	1000	2016-12-18	2020-03-05	3.2	GrPlains
NEON.D10.ARIK.	39.76	-102.45	GR	1000	2016-12-18	2020-03-05	3.1	GrPlains
NEON.D10.CPER.	40.82	-104.75	GR	1000	2016-06-30	2020-03-05	3.7	GrPlains
NEON.D10.STER.	40.46	-103.03	AG	1000	2016-12-18	2020-03-05	3.2	GrPlains
NEON.D11.OAES.	35.41	-99.06	GR	1000	2017-02-28	2020-03-05	3.0	GrPlains
NEON.D13.MOAB.	38.25	-109.39	GR	1000	2017-02-25	2020-03-05	3.0	NADeserts
NEON.D14.JORN.	32.59	-106.84	GR	1000	2017-02-25	2020-03-05	3.0	NADeserts
NEON.D14.SRER.	31.91	-110.84	SH	1000	2017-02-25	2020-03-05	3.0	NADeserts
NEON.D15.ONAQ.	40.18	-112.45	GR	1000	2016-12-18	2020-03-05	3.2	NADeserts
NEON.D15.ONAQ.	40.18	-112.45	SH	1001	2016-12-18	2020-03-05	3.2	NADeserts
oakville	47.90	-97.32	GR	1000	2014-08-06	2020-03-05	4.6	GrPlains

Table A3. Sites used continued

name	lat	lon	vegetation	roi id	first date	last date	site years	ecoregion
pointreyes	38.00	-123.02	SH	1000	2004-01-23	2019-03-18	13.3	MedCA
rosemountnprs	44.68	-93.07	AG	1000	2015-10-29	2020-03-05	4.3	GrPlains
sevilletagrass	34.36	-106.70	GR	1000	2014-11-07	2020-03-05	5.1	NADeserts
sevilletashrub	34.33	-106.74	SH	1000	2014-10-29	2020-03-05	5.0	NADeserts
silverton	45.00	-122.69	AG	1000	2013-07-22	2020-02-10	5.9	NWForests
smokypurchase	35.59	-83.07	GR	2000	2016-01-02	2020-03-05	4.0	ETempForests
southerngreatplains	36.61	-97.49	AG	1000	2012-05-16	2020-03-05	7.5	GrPlains
spruceT6P16E	47.51	-93.45	SH	1000	2015-08-24	2020-03-05	4.6	NForest
stjones	39.09	-75.44	GR	1000	2015-09-20	2020-03-05	4.4	ETempForests
sweetbriargrass	37.56	-79.09	AG	1000	2016-03-23	2020-03-05	3.8	ETempForests
teddy	46.89	-103.38	GR	1000	2010-01-02	2019-03-27	8.5	GrPlains
teddy	46.89	-103.38	SH	1000	2003-05-11	2019-03-27	14.4	GrPlains
tonzi*	38.43	-120.97	GR	1000	2011-10-26	2020-02-13	7.3	MedCA
turkeypointenf02	42.66	-80.56	AG	1000	2012-05-01	2020-03-05	7.5	ETempForests
twitchell	38.11	-121.65	AG	1000	2011-11-16	2017-04-05	4.0	MedCA
uiefmaize	40.06	-88.20	AG	1000	2008-11-06	2020-03-02	11.3	ETempForests
uiefmiscanthus	40.06	-88.20	AG	1000	2008-11-12	2018-04-29	9.2	ETempForests
uiefprairie*	40.06	-88.20	GR	1000	2008-10-22	2020-03-02	11.3	ETempForests
uiefswitchgrass	40.06	-88.20	AG	1000	2008-10-22	2020-03-02	10.6	ETempForests
usgseros	43.73	-96.62	GR	1000	2014-09-11	2017-10-02	3.1	GrPlains
uwmfieldsta	43.39	-88.02	GR	1000	2013-03-15	2020-03-05	7.0	ETempForests
vaira*	38.41	-120.95	GR	1000	2011-10-17	2020-02-28	7.7	MedCA

References

Adams, J. M., Faure, H., Faure-Denard, L., McGlade, J. M., and Woodward, F. I.: Increases in terrestrial carbon storage from the Last Glacial Maximum to the present, Nature, 348, 711–714, https://doi.org/10.1038/348711a0, 1990.

Basler, D.: Evaluating phenological models for the prediction of leaf-out dates in six temperate tree species across central Europe, Agricultural and Forest Meteorology, 217, 10–21, https://doi.org/10.1016/j.agrformet.2015.11.007, 2016.

Bégué, A., Arvor, D., Bellon, B., Betbeder, J., de Abelleyra, D., P. D. Ferraz, R., Lebourgeois, V., Lelong, C., Simões, M., and R. Verón, S.: Remote Sensing and Cropping Practices: A Review, Remote Sensing, 10, 99, https://doi.org/10.3390/rs10010099, 2018.

Bivand, R., Keitt, T., and Rowlingson, B.: rgdal: Bindings for the 'Geospatial' Data Abstraction Library, https://cran.r-project.org/package=rgdal, 2019.

Browning, D. M., Maynard, J. J., Karl, J. W., and Peters, D. C.: Breaks in MODIS time series portend vegetation change: verification using long-term data in an arid grassland ecosystem, Ecological Applications, 27, 1677–1693, https://doi.org/10.1002/eap.1561, 2017.

Choler, P., Sea, W., Briggs, P., Raupach, M., and Leuning, R.: A simple ecohydrological model captures essentials of seasonal leaf dynamics in semi-arid tropical grasslands, Biogeosciences, 7, 907–920, https://doi.org/10.5194/bg-7-907-2010, 2010.

Choler, P., Sea, W., and Leuning, R.: A Benchmark Test for Ecohydrological Models of Interannual Variability of NDVI in Semi-arid Tropical Grasslands, Ecosystems, 14, 183–197, https://doi.org/10.1007/s10021-010-9403-9, 2011.

Donohue, R. J., Roderick, M. L., McVicar, T. R., and Farquhar, G. D.: Impact of CO 2 fertilization on maximum foliage cover across the globe's warm, arid environments, Geophysical Research Letters, 40, 3031–3035, https://doi.org/10.1002/grl.50563, 2013.

Easterling, D. R., Kunkel, K., Arnold, J., Knutson, T. R., LeGrande, A., Leung, L., Vose, R. S., Waliser, D., and Wehner, M.: Precipitation change in the United States, in: Climate Science Special Report: Fourth National Climate Assessment, Volume I, vol. I, pp. 207–230, U.S. Global Change Research Program, Washington, D.C., USA, https://doi.org/10.7930/J0H993CC.U.S., 2017.

Fritz, S., See, L., Bayas, J. C. L., Waldner, F., Jacques, D., Becker-Reshef, I., Whitcraft, A., Baruth, B., Bonifacio, R., Crutchfield, J., Rembold, F., Rojas, O., Schucknecht, A., Van der Velde, M., Verdin, J., Wu, B., Yan, N., You, L., Gilliams, S., Mücher, S., Tetrault, R., Moorthy, I., and McCallum, I.: A comparison of global agricultural monitoring systems and current gaps, Agricultural Systems, 168, 258–272, https://doi.org/10.1016/j.agsy.2018.05.010, 2019.

García-Mozo, H., Chuine, I., Aira, M., Belmonte, J., Bermejo, D., Díaz de la Guardia, C., Elvira, B., Gutiérrez, M., Rodríguez-Rajo, J., Ruiz, L., Trigo, M., Tormo, R., Valencia, R., and Galán, C.: Regional phenological models for forecasting the start and peak of the Quercus pollen season in Spain, Agricultural and Forest Meteorology, 148, 372–380, https://doi.org/10.1016/j.agrformet.2007.09.013, 2008.

Global Soil Data Task Group: Global Gridded Surfaces of Selected Soil Characteristics (IGBP-DIS), https://doi.org/10.3334/ORNLDAAC/569, 2000.

Hargreaves, G. H. and Samani, Z. A.: Reference Crop Evapotranspiration from Temperature, Applied Engineering in Agriculture, 1, 96–99, https://doi.org/10.13031/2013.26773, 1985.

Hufkens, K., Keenan, T. F., Flanagan, L. B., Scott, R. L., Bernacchi, C. J., Joo, E., Brunsell, N. A., Verfaillie, J., and Richardson, A. D.: Productivity of North American grasslands is increased under future climate scenarios despite rising aridity, Nature Climate Change, 6, 710–714, https://doi.org/10.1038/nclimate2942, 2016.

Hufkens, K., Basler, D., Milliman, T., Melaas, E. K., and Richardson, A. D.: An integrated phenology modelling framework in <scp>r</scp>, Methods in Ecology and Evolution, 9, 1276–1285, https://doi.org/10.1111/2041-210X.12970, 2018.

Knapp, A. K., Ciais, P., and Smith, M. D.: Reconciling inconsistencies in precipitation-productivity relationships: implications for climate change, New Phytologist, 214, 41–47, https://doi.org/10.1111/nph.14381, 2017.

Lauenroth, W. K., Schlaepfer, D. R., and Bradford, J. B.: Ecohydrology of Dry Regions: Storage versus Pulse Soil Water Dynamics, Ecosystems, 17, 1469–1479, https://doi.org/10.1007/s10021-014-9808-y, 2014.

McKinney, W.: Data Structures for Statistical Computing in Python, in: Proceedings of the 9th Python in Science Conference, pp. 51–56, SciPy, Austin, Texas, USA, http://conference.scipy.org/proceedings/scipy2010/mckinney.html, 2010.

Muldavin, E. H., Moore, D. I., Collins, S. L., Wetherill, K. R., and Lightfoot, D. C.: Aboveground net primary production dynamics in a northern Chihuahuan Desert ecosystem, Oecologia, 155, 123–132, https://doi.org/10.1007/s00442-007-0880-2, 2008.

Ogle, K. and Reynolds, J. F.: Plant responses to precipitation in desert ecosystems: integrating functional types, pulses, thresholds, and delays, Oecologia, 141, 282–294, https://doi.org/10.1007/s00442-004-1507-5, 2004.

Omernik, J. M. and Griffith, G. E.: Ecoregions of the Conterminous United States: Evolution of a Hierarchical Spatial Framework, Environmental Management, 54, 1249–1266, https://doi.org/10.1007/s00267-014-0364-1, 2014.

Parton, W., Morgan, J., Smith, D., Del Grosso, S., Prihodko, L., LeCain, D., Kelly, R., and Lutz, S.: Impact of precipitation dynamics on net ecosystem productivity, Global Change Biology, 18, 915–927, https://doi.org/10.1111/j.1365-2486.2011.02611.x, 2012.

Pebesma, E.: Simple Features for R: Standardized Support for Spatial Vector Data, The R Journal, 10, 439–446, https://doi.org/10.32614/RJ-2018-009, 2018.

Richardson, A. D., Hufkens, K., Milliman, T., Aubrecht, D. M., Chen, M., Gray, J. M., Johnston, M. R., Keenan, T. F., Klosterman, S. T., Kosmala, M., Melaas, E. K., Friedl, M. A., and Frolking, S.: Tracking vegetation phenology across diverse North American biomes using PhenoCam imagery, Scientific Data, 5, 180 028, https://doi.org/10.1038/sdata.2018.28, 2018a.

Richardson, A. D., Hufkens, K., Milliman, T., and Frolking, S.: Intercomparison of phenological transition dates derived from the PhenoCam Dataset V1.0 and MODIS satellite remote sensing, Scientific Reports, 8, 5679, https://doi.org/10.1038/s41598-018-23804-6, 2018b.

Ritter, A. and Muñoz-Carpena, R.: Performance evaluation of hydrological models: Statistical significance for reducing subjectivity in goodness-of-fit assessments, Journal of Hydrology, 480, 33–45, https://doi.org/10.1016/j.jhydrol.2012.12.004, 2013.

Sala, O. E., Gherardi, L. A., Reichmann, L., Jobbagy, E., and Peters, D.: Legacies of precipitation fluctuations on primary production: theory and data synthesis, Philosophical Transactions of the Royal Society B: Biological Sciences, 367, 3135–3144, https://doi.org/10.1098/rstb.2011.0347, 2012.

Scanlon, T. M., Caylor, K. K., Manfreda, S., Levin, S. A., and Rodriguez-Iturbe, I.: Dynamic response of grass cover to rainfall variability: implications for the function and persistence of savanna ecosystems, Advances in Water Resources, 28, 291–302, https://doi.org/10.1016/j.advwatres.2004.10.014, 2005.

Seyednasrollah, B., Young, A. M., Hufkens, K., Milliman, T., Friedl, M. A., Frolking, S., and Richardson, A. D.: Tracking vegetation phenology across diverse biomes using Version 2.0 of the PhenoCam Dataset, Scientific data, 6, 222, https://doi.org/10.1038/s41597-019-0229-9, 2019.

Taylor, S. D., Meiners, J. M., Riemer, K., Orr, M. C., and White, E. P.: Comparison of large-scale citizen science data and long-term study data for phenology modeling, Ecology, 100, e02 568, https://doi.org/10.1002/ecy.2568, 2019.

Team, D. D.: Dask: Library for dynamic task scheduling, https://dask.org, 2016.

Thornton, P. E., Thornton, M. M., Mayer, B. W., Wei, Y., Devarakonda, R., Vose, R., and Cook, R. B.: Daymet: Daily Surface Weather Data on a 1-km Grid for North America, Version 3., Tech. rep., ORNL DAAC, Oak Ridge, Tennessee, USA, Oak Ridge, Tennessee, USA, https://doi.org/10.3334/ORNLDAAC/1328, 2018.

Toomey, M., Friedl, M. A., Frolking, S., Hufkens, K., Klosterman, S., Sonnentag, O., Baldocchi, D. D., Bernacchi, C. J., Biraud, S. C., Bohrer, G., Brzostek, E., Burns, S. P., Coursolle, C., Hollinger, D. Y., Margolis, H. A., McCaughey, H., Monson, R. K., Munger, J. W., Pallardy, S., Phillips, R. P., Torn, M. S., Wharton, S., Zeri, M., and Richardson, A. D.: Greenness indices from digital cameras predict the timing and seasonal dynamics of canopy-scale photosynthesis, Ecological Applications, 25, 99–115, https://doi.org/10.1890/14-0005.1, 2015.

van der Walt, S., Colbert, S. C., and Varoquaux, G.: The NumPy Array: A Structure for Efficient Numerical Computation, Computing in Science and Engineering, 13, 22–30, https://doi.org/10.1109/MCSE.2011.37, 2011.

Virtanen, P., Gommers, R., Oliphant, T. E., Haberland, M., Reddy, T., Cournapeau, D., Burovski, E., Peterson, P., Weckesser, W., Bright, J., van der Walt, S. J., Brett, M., Wilson, J., Millman, K. J., Mayorov, N., Nelson, A. R. J., Jones, E., Kern, R., Larson, E., Carey, C. J., Polat, I., Feng, Y., Moore, E. W., VanderPlas, J., Laxalde, D., Perktold, J., Cimrman, R., Henriksen, I., Quintero, E. A., Harris, C. R., Archibald, A. M., Ribeiro, A. H., Pedregosa, F., and van Mulbregt, P.: SciPy 1.0: fundamental algorithms for scientific computing in Python, Nature Methods, 17, 261–272, https://doi.org/10.1038/s41592-019-0686-2, 2020.

Weltzin, J. F. and McPherson, G. R.: Implications of precipitation redistribution for shifts in temperate savanna ecotones, Ecology, 81, 1902–1913, 2000.

Wickham, H.: ggplot2: Elegant Graphics for Data Analysis, Springer-Verlag New York, http://ggplot2.org, 2016.

Wickham, H. and Henry, L.: tidyr: Easily Tidy Data with 'spread()' and 'gather()' Functions, https://cran.r-project.org/package=tidyr, 2018.

Wickham, H., Francois, R., Henry, L., and Müller, K.: dplyr: A Grammar of Data Manipulation, https://cran.r-project.org/package=dplyr, 2017.

Yan, D., Scott, R., Moore, D., Biederman, J., and Smith, W.: Understanding the relationship between vegetation greenness and productivity across dryland ecosystems through the integration of PhenoCam, satellite, and eddy covariance data, Remote Sensing of Environment, 223, 50–62, https://doi.org/10.1016/j.rse.2018.12.029, 2019.

Zhang, L., Wylie, B. K., Ji, L., Gilmanov, T. G., Tieszen, L. L., and Howard, D. M.: Upscaling carbon fluxes over the Great Plains grasslands: Sinks and sources, Journal of Geophysical Research: Biogeosciences, 116, 1–13, https://doi.org/10.1029/2010JG001504, 2011.